Slow-particle-induced kinetic electron emission from a clean metal surface: A comparison for neutral and ionized projectiles

G. Lakits, A. Arnau,* H. Winter
Institut für Allgemeine Physik, Technische Universität Wien, Wiedner Haupstrasse 8-10, A-1040 Wien, Austria
(Received 29 December 1989)

Electron emission from a clean gold surface bombarded by slow ($v < 1$ a.u.) neutral or singly charged atoms has been investigated both experimentally and theoretically. The determination of electron-emission statistics for 1–16-keV H^+, H^0, H^-, He^+, He^0, Ne^+, Ne^0, Ar^+, and Ar^0, respectively, delivered accurate total electron-emission yields, which are consistently higher for positively charged ions than for the corresponding isoenergetic neutral atoms. It was assured that potential emission could not be responsible for the observed differences. H^- bombardment at low impact energy causes equal yields as for H^0, but for higher kinetic energy even the yields for H^+ are surpassed. The results are explained with a semiempirical theory for heavy-particle-induced electron emission, assuming different screening of projectile cores by the accompanying electron(s) during the continuous change of projectile charge upon penetration of the solid. For H^+,H^0 bombardment a quantitative description of the experimentally observed effects could be achieved by calculation of the stopping power for slow projectiles in different charge states, together with the electron-capture and -loss cross sections for these projectiles colliding with the target atoms.

I. INTRODUCTION

Bombardment of metal surfaces with slow heavy particles (neutral or ionized atoms) causes electron emission, which is of considerable relevance, e.g., for plasma-solid interaction, gaseous electronics, or single-particle detection. Although such processes have already been studied for about a century,[1] up till now the underlying mechanisms have still not been sufficiently well understood.

Particle-induced electron emission is commonly related to two different mechanisms. Potential emission (PE) occurs for positive ion bombardment already at the lowest impact velocity, if the potential energy of the ion exceeds twice the work function of the metal surface.[2] Kinetic emission (KE) is also observed for neutral atoms as soon as a threshold projectile velocity of typically 10^5 ms^{-1} is surpassed.[3]

At impact velocities well below 1 a.u. the two emission processes are usually assumed to act independently of each other, because the PE is already terminated before the projectiles reach the surface to initiate KE processes.

The aim of this paper is to show that in cases where a projectile has not been fully neutralized before hitting the surface, the KE yields will depend on the initial projectile charge state. In Sec. II we discuss recent theories on KE[4] and present calculations of the relevant electronic stopping power in the low-energy regime. Measured differences in total electron emission yields for differently charged projectiles are discussed within a semiempirical theory for heavy-particle-induced electron emission.[5] For the particular case of H^+, H^0 colliding with clean gold, this discussion is based on calculations of electron-capture and -loss cross sections, to obtain the actual charge state of projectiles penetrating the uppermost layers of the target.

In Sec. III we derive total electron emission yields from electron emission statistics[6] measured for bombardment of a clean gold surface with either ionized or neutral atoms. This technique permits a more precise comparison of the electron emission yields than current measurements and/or calorimetric methods. Experimental results for 1–16 keV H^+, H^0, H^-, He^+, He^0, Ne^+, Ne^0, Ar^+, and Ar^0, respectively, are presented in Sec. IV and compared with the theoretical predictions from Sec. II.

II. THEORETICAL BACKGROUND ON SLOW PARTICLE-INDUCED ELECTRON EMISSION FROM METAL SURFACES

A. Potential electron emission

In the context of this paper, potential emission is defined as electron emission occurring before the projectiles hit the surface. For PE induced by singly charged ion bombardment, Auger neutralization and/or resonance neutralization followed by Auger deexcitation are the primarily responsible processes.[2] The probabilities for these processes can be calculated from the overlap between the wave functions of involved projectile states and the target surface density of states.

For PE to become possible the potential energy W_q of the approaching ion has to exceed twice the work function Φ of the target metal. For the total PE yield γ_P the following semiempirical dependence on the potential energy of the ion has been given[3] (atomic units are used throughout this work except where otherwise stated)

$$\gamma_P = \frac{0.2}{\varepsilon_F}(0.8 W_q - 2\Phi) \quad (1)$$

with ε_F the Fermi energy of the target.

This formula does not involve the projectile velocity and therefore delivers an upper limit, characteristic for low-impact velocities, since with increasing impact velocity the PE yield decreases in accordance with the decreasing time for passing the region in front of the surface, in which ion neutralization or deexcitation can take place. Therefore, the higher the projectile velocity, the more probably it will hit the surface in still ionized state.

B. Kinetic electron emission

Recent theories describe heavy particle-induced electron emission within a multistep model covering the following scenario.

(i) Primary ionization of target atoms via direct (screened) Coulomb interaction with the projectile.

(ii) Secondary ionization of target atoms by recoiling target atoms, energetic electrons, and possibly photons.

(iii) Transport of the liberated electrons toward the surface.

(iv) Penetration of electrons through the surface barrier into vacuum.

Schou[4] gives the following dependence of the total electron emission yield γ_K on the projectile kinetic energy E:

$$\gamma_K = \Lambda D(E) \ . \tag{2}$$

Here Λ is a target-dependent constant describing transport of the electrons inside the solid and their ejection through the surface barrier. Λ can be determined either by solving an electron transport equation or from comparison with experiment. $D(E)$ describes the production mechanisms for electrons. For heavy target atoms bombarded by light projectiles the contribution from recoil atoms is negligible. In particular, for low-projectile velocity the primary ionization is dominant, and $D(E)$ will therefore be proportional to the ionization cross section σ_I of the target atoms. At higher impact velocity, the electrons are also produced from cascades induced by energetic primary electrons, and $D(E)$ becomes thus proportional to the electronic stopping power S_e of the projectile. If the projectile and target masses are comparable, energetic recoil atoms contribute as well to the electron production, and a term proportional to the nuclear stopping cross section has to be added.

A simplified semiempirical model of KE has been developed by Baragiola *et al.*[5] They assumed the electron production to result from binary collisions involving screened Coulomb interaction between the projectile and the quasifree target electrons. An impact velocity threshold $v_{\rm th}$ for KE can be obtained from the maximum energy transfer surpassing the target work function Φ

$$v_{\rm th} = \frac{1}{2} v_F \left[\left[1 + \frac{2\Phi}{m v_F^2} \right]^{1/2} - 1 \right] , \tag{3}$$

where v_F is the Fermi velocity of the target electrons. Equation (3) is only valid for bombardment with light projectiles, whereas for heavier projectiles carrying a number of electrons the electron promotion mechanism contributes to electron production already at much lower velocities than predicted by Eq. (3). Consequently, $v_{\rm th}$ defines an upper limit for the KE velocity threshold.

Calculation of the total electron yield from this semiempirical theory is based on the assumption that the mean energy J for creating an electron-hole pair, with the final electron energy being above the vacuum level, is independent of the projectile velocity. Then the number $N(x)$ of ionized electrons in the depth interval $[x, x+dx]$ can be expressed by

$$N(x) = \frac{S_e(x,E)}{J} dx \tag{4a}$$

with $S_e = -dE/dx$ being the electronic stopping power. Transport of electrons toward the surface is taken care of by an exponential attenuation function of the electron flux over a mean length L, which is smaller than the mean free path of electrons λ, when taking into account the contributions from the half solid angle directed toward the surface.

With P being the probability for an electron to overcome the surface potential barrier, one obtains for the total electron emission yield γ_K at a given ion impact energy E

$$\gamma_K(E) = \frac{P}{2J} \int_0^\infty S_e(x,E) e^{-x/L} dx \ . \tag{4b}$$

For projectile velocities well above the threshold [cf. Eq. (3)] one can assume that a projectile looses only a small fraction of its energy along the mean electron escape depth L, and thus $S_e(x,E) \approx S_e(0,E)$, for which the integral in Eq. (4b) can easily be solved, with γ_K becoming proportional to the electronic stopper power[4] as obtained for bombardment of heavy targets with light projectiles.

However, for KE induced by ionized projectiles this approximation is not valid because the projectile charge state changes during penetration of the solid and thus a variation of stopping power has to be taken into account. An adequate treatment for such cases will be presented in the following sections.

C. Change of projectile charge state during penetration of solids

We assume that projectiles change their state when penetrating the solid in a similar way as in collisions with a gas target, for which the processes can be described by a system of differential equations:

$$\frac{1}{n} \frac{dF_0}{dx} = \sigma_{10} F_1 - \sigma_{01} F_0 \ , \tag{5a}$$

$$\frac{1}{n} \frac{dF_1}{dx} = \sigma_{01} F_0 - \sigma_{10} F_1 \ . \tag{5b}$$

Here n is the atomic number density of the target, F_0 and F_1 are the fractions of neutral and singly charged atoms in the beam, σ_{01} and σ_{10} the loss and capture cross sections, and x is the depth below the target surface, respectively. Appearance of negative as well as multiply charged ion fractions is neglected. In particular, the neglect of H^- formation is reasonable for a high electron

density material like gold, because of the efficient screening by the valence electrons. However, H^- formation should probably not be neglected in materials with a lower electron density, e.g., alkali metals or aluminum.[8]

Equation (5) is solved by taking into account the continuity condition $F_0(x)+F_1(x)\equiv 1$ and the initial conditions $F_1(0)=1$ for singly charged ion impact and $F_0(0)=1$ for neutral atom impact, respectively. Consequently, F_1 is given by Eq. (6a) for initially singly charged ions and Eq. (6b) for initially neutral atoms, from which the corresponding values for $F_0(x)$ can be derived:

$$F_1^+(x)=1-F_0^\infty(1-e^{-x/x_0}) , \tag{6a}$$

$$F_1^0(x)=(1-F_0^\infty)(1-e^{-x/x_0}) , \tag{6b}$$

where F_0^∞ is the equilibrium charge state fraction resulting for $x\rightarrow\infty$,

$$F_0^\infty=\frac{\sigma_{10}}{\sigma_{10}+\sigma_{01}} \tag{6c}$$

and x_0 the corresponding e-folded length

$$x_0=\frac{1}{n}\frac{1}{\sigma_{10}+\sigma_{01}} . \tag{6d}$$

Unfortunately, measured charge-changing cross sections σ_{01} and σ_{10} for gold are not available to check the accuracy of Eqs. (6). Therefore, for the particular case of H^+/H^0 bombardment of gold we have calculated such cross sections by applying a simple model, the details of which are presented in Sec. II E. The obtained results also permit calculation of the equilibrium charge state fractions F_i^∞ and the e-folded length x_0.

Figure 1 shows calculated charge fractions F_1^+ and F_1^0 for bombardment with 16-keV H^+ and H^0 projectiles, respectively (cf. Sec. III E). From the difference of these fractions within a typical electron escape length $L\approx 2$ nm we explain our observed differences for particle-induced electron emission, as will be further discussed in Sec. IV.

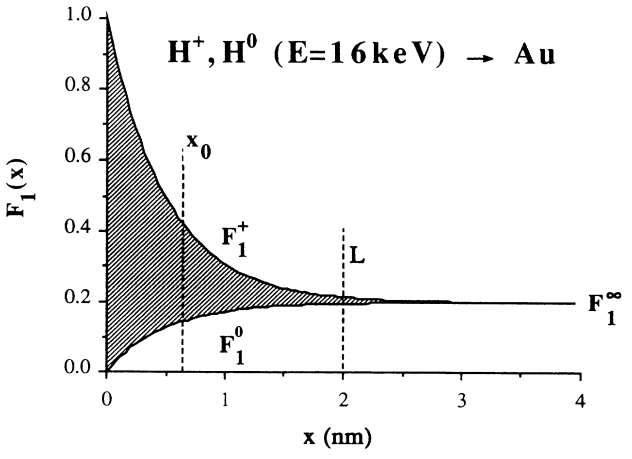

FIG. 1. Ionized projectile fraction F_1^+ for 16-keV proton (upper curve) and H atom (F_1^0, lower curve) bombardment of gold, depending on the depth of penetration.

D. Electronic effects in particle-induced electron emission

With the above described concept of charge-changing collisions inside a solid we now modify the semiempirical formula (4a) for particle-induced kinetic electron emission. Instead of the electronic stopping power $S_e(0,E)$ we introduce a depth-dependent function $S_e(x,E)$, which takes into account the changing charge state fractions F_0 and F_1 as derived above:

$$S_e(x,E)\equiv F_0(x)S_0(E)+F_1(x)S_1(E). \tag{7a}$$

$S_1(E)$ is the electronic stopping power for singly charged ions. In Eq. (7a) we have neglected a contribution to the stopping power from the charge exchange processes because it is very small at low velocities.[8] For neutral projectiles we assume their interaction with the target electrons to be screened by the accompanying electron according to a factor $k<1$. Therefore, the stopping power $S_0(E)$ for the (screened) neutral projectile is expressed as

$$S_0(E)\equiv kS_1(E) . \tag{7b}$$

Inserting Eqs. (7) into Eq. (4b) one obtains the ratio of yields for bombardment by neutral and singly charged projectiles, respectively,

$$\frac{\gamma^0}{\gamma^+}=\frac{(1-F_0^\infty)(1-k)+k(1+y)}{(1-F_0^\infty)(1-k)+k+y} \tag{8a}$$

with y defined as

$$y\equiv\frac{x_0}{L} . \tag{8b}$$

In the here investigated impact energy regime $E\leq 16$ keV the capture cross section is much larger than the loss cross section (cf. Sec. II E), i.e., $\sigma_{10}\gg\sigma_{01}$ and therefore $F_0^\infty\approx 1$. In this case γ^0/γ^+ can be approximated by

$$\frac{\gamma^0}{\gamma^+}\approx\frac{k(1+y)}{k+y} . \tag{8c}$$

Another remarkable prediction of Eq. (8a) is that in the limit $x_0\gg L$, i.e., $y\gg 1$ the yield ratio γ^0/γ^+ should approach the screening factor k, as will be the case for low-electron-density materials.

We observe that Eqs. (8) predict the independence of the ratio γ^0/γ^+ not only of the target parameters P and J, but also of the stopping power S_e. By knowing k and the ratio y one can therefore easily calculate γ^0/γ^+. In Sec. IV B we compare such calculations with our measurements for H^+, H^0 bombardment.

E. Calculation of electron capture and loss cross sections for protons in gold

In the low-impact energy regime ($E<25$ keV/amu or $v<v_0$ with $v_0\equiv 1$ a.u. being the Bohr velocity), two mechanisms are responsible for electron capture and loss of the projectiles moving through the solid. These are the interaction with the lattice ion core periodic potential and the interaction with the conduction-band electrons. The tightly bound electrons in the inner shells of the Au

cores are "frozen" in the sense that they do not contribute to the capture cross section.

In the frame of reference of the moving proton, together with its possibly bound electron it feels a time-dependent periodic potential due to the passing of the lattice ion cores with a characteristic frequency $\omega \approx v/a$, where a is the lattice constant. In first order time-dependent perturbation theory each Fourier component $V(\mathbf{G})$ of the potential ($\mathbf{G}$ is a reciprocal lattice vector) contributes to a transition between electronic states in the target and a bound state in the moving proton, if the energy change $\omega = \mathbf{G}\cdot\mathbf{v}$ matches the excitation energy between electronic levels. We have used an Ashcroft pseudopotential[9] to characterize the interaction of the electronic levels with the lattice ion cores. The capture (σ_{10}) and loss (σ_{01}) cross sections can be obtained from the probability per unit time for capturing (Γ_C) or loosing (Γ_L) an electron through the relations

$$\sigma_{01} = \frac{\Gamma_L}{nv} \quad \text{and} \quad \sigma_{10} = \frac{\Gamma_C}{nv} , \tag{9a}$$

where n is the atomic density of the target and $\Gamma_{C,L}$ are given by[10]

$$\Gamma_{C,L} = 2\pi \nu_{C,L} \sum_{\mathbf{G}} \sum_{|\mathbf{k}+\mathbf{v}| <, > k_F} |V(\mathbf{G})|^2 |\langle s | e^{i\mathbf{G}\cdot\mathbf{r}} | \mathbf{k} \rangle|^2 \delta(E_{k0} +, -\mathbf{G}\cdot\mathbf{v}) . \tag{9b}$$

$\nu_{C,L} = 2, 1$ takes into account the spin degeneracy in the capture process and $E_{k0} = (k^2/2) - E_b$, with E_b the binding energy of the electron to the proton in H^0. $|s\rangle$ denotes the electron state bound to the proton that we have considered as a variational $1s$ hydrogenlike wave function, determined by a minimization procedure.[11] $|\mathbf{k}\rangle$ denotes an electron state in the conduction band that has been approximated by a plane wave orthogonalized to the $|s\rangle$ state. The summation over $|\mathbf{k}\rangle$ states takes into account the Pauli exclusion principle and the shift in velocity space of the Fermi sphere in the frame of reference of the moving proton through the relations $|\mathbf{k}+\mathbf{v}| <$ and $> k_F$ for the capture and loss processes, respectively.

Due to the interaction with the electrons in the conduction band, direct capture to (and loss from) the bound state of the moving proton from (to) electron states in the conduction band may also occur assisted by the creation of an elementary excitation (mainly electron-hole pairs) in the target. We have calculated the capture and loss cross sections for such processes from the imaginary part of the self-energy (Σ) associated with the proton-bound electron composite [$\Gamma = -2\,\mathrm{Im}(\Sigma)$].[11] The complicated electronic structure of gold has been treated by using a simple model that takes into account the excitation of the conduction band electrons with a dielectric function $\varepsilon(q,\omega)$, with the latter being approximated by experimentally obtained[12] optical data $\varepsilon(\omega)$ with a cutoff in wave vector space $q_c = 1$. The probabilities per unit time of capturing or loosing the electron by the proton in this case are given by[13]

$$\Gamma_{C,L} = 2\nu_{C,L} \sum_{\mathbf{k}+\mathbf{v}| <, > k_F} \int d\omega \int \frac{d\mathbf{q}}{(2\pi)^3} \frac{4\pi}{q^2} \mathrm{Im}\left[\frac{-1}{\varepsilon(q,\omega)}\right] |M_{\mathbf{k}0}|^2 \delta(\omega -, +\Delta E) , \tag{9c}$$

where $M_{\mathbf{k}0} = \langle s | e^{iqr} | \mathbf{k} \rangle$ and $\Delta E = \mathbf{q}\cdot\mathbf{v} + E_b + (k^2/2)$. $\mathrm{Im}(x)$ denotes the imaginary part of x, with the other symbols already having been defined.

The such obtained cross sections for capture σ_{10} and loss σ_{01} for protons in Au are shown in Figs. 2(a) and 2(b) versus the impact energy E of the moving proton. In the range 1 keV $\leq E \leq$ 16 keV ($0.2 \leq v/v_0 \leq 0.8$) the typical equilibrium lengths x_0 to achieve the equilibrium charge states are in the range of 7 Å $\leq x_0 \leq$ 5 Å. The capture cross sections are considerably larger than the loss cross sections in this energy range and therefore the neutral equilibrium fraction F_0^∞ is bigger than that of the bare protons F_1^∞. The two equilibrium fractions become roughly equal at $E = 25$ keV.

F. Calculation of low-velocity stopping power for protons and hydrogen atoms

If the ion velocity is small compared with the Fermi velocity v_F of the electrons in the target, the stopping power can be expressed[14] as

$$\frac{dE}{dx} = nvv_F \sigma_{\mathrm{tr}}(E_F) , \tag{10a}$$

where $n = v_F^3/(3\pi^2)$ is the homogeneous electron density of the idealized metal and $\sigma_{\mathrm{tr}}(E_F)$ is the momentum-transfer cross section at the Fermi level. This can be written in terms of the phase shifts $\delta_l(E_F)$ for scattering of electrons at the Fermi level by a statically screened spherically symmetric potential (for heavy ions at low velocities the screening can be regarded as static) as

$$\sigma_{\mathrm{tr}}(E_F) = \frac{4\pi}{v_F^2} \sum_{l=0}^{\infty} (l+1) \sin^2(\delta_l - \delta_{l+1}) . \tag{10b}$$

As a first approach we have determined the scattering potential by linearly screening, with a Thomas-Fermi

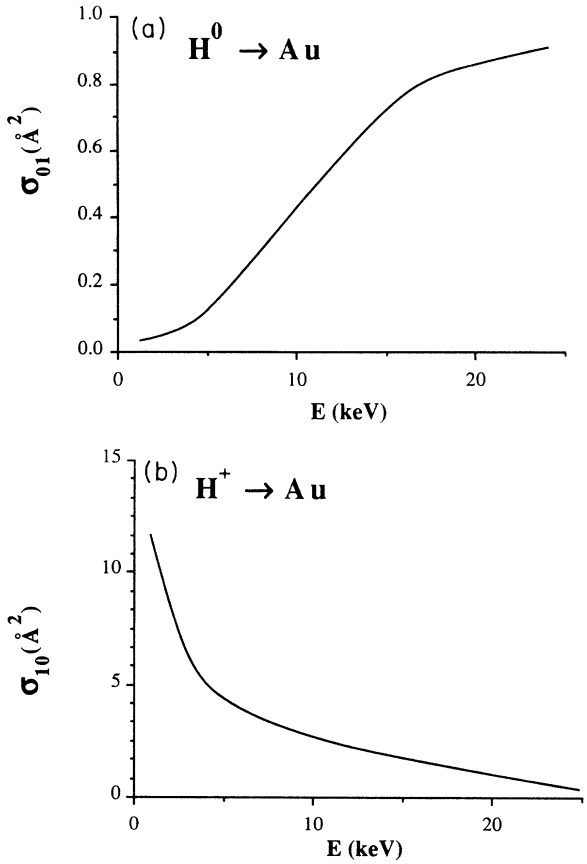

FIG. 2. (a) Electron loss cross sections σ_{01} for H atoms moving in Au vs projectile energy E. (b) Electron capture cross sections σ_{10} for protons moving in Au vs projectile energy E.

dielectric function, the bare potential created by a point charge in the case of H^+ or a point charge with a spherically symmetric charge density around it in the case of H^0. In this way we obtain the potential in real space $V(r)$ needed in the radial Schrödinger equation of the scattering problem by a simple Fourier transform

$$V(r)=\int \frac{d\mathbf{q}}{(2\pi)^3} e^{i\mathbf{q}\cdot\mathbf{r}} V(q) , \tag{11a}$$

where

$$V(q)=\frac{4\pi\rho(q)}{q^2\varepsilon(q)} \quad \text{and} \quad \varepsilon(q)=1+\frac{\lambda^2}{q^2} \tag{11b}$$

$\rho(q)=Z_1$ for a bare charge and $Z_1-n_b(q)$ for a bare charge Z_1 with a spherically symmetric charge density $n_b(r)$ around it, $n_b(q)$ being the Fourier transform of $n_b(r)$. The parameter λ in the Thomas-Fermi dielectric function is given by $\lambda=(4v_F/\pi)^{1/2}$. For the proton we take $Z_1=1$ and for the hydrogen atom $Z_1=1$ and

$$n_b(q)=\left[1+\left[\frac{q}{2\alpha}\right]^2\right]^{-2} \tag{11c}$$

with α the parameter of a 1s-type wave function.

The final form of the potentials $V(r)$ is of the well-known Yukawa type for the proton, whereas for the hydrogen atom one obtains

$$V(r)=-\frac{Z_1}{r}e^{-\lambda r} + \frac{16\alpha^4}{(4\alpha^2-\lambda^2)^2}\left[\frac{e^{-\lambda r}}{r} - \frac{e^{-2\alpha r}}{r}\left[1+\frac{4\alpha^2-\lambda^2}{4\alpha}r\right]\right] . \tag{11d}$$

The results which we have obtained for the stopping power of slow protons and hydrogen atoms are plotted as a function of the density parameter $r_s(r_s=1.92/v_F)$ in Fig. 3(a). At low electron densities (high r_s values) there is roughly a factor of 5 between the stopping power for H^+ and for H^0. In the typical metallic density range ($1.5\leq r_s\leq 2$) the stopping power for H^0 is about 50–70 % of that for H^+. Note, however, that at higher electron densities (smaller r_s) the bound state will not appear at all. The ratio of the stopping power for H^0 to that for H^+ has been plotted as a function of r_s in Fig. 3(b). The agreement of the results that we obtain in this simple

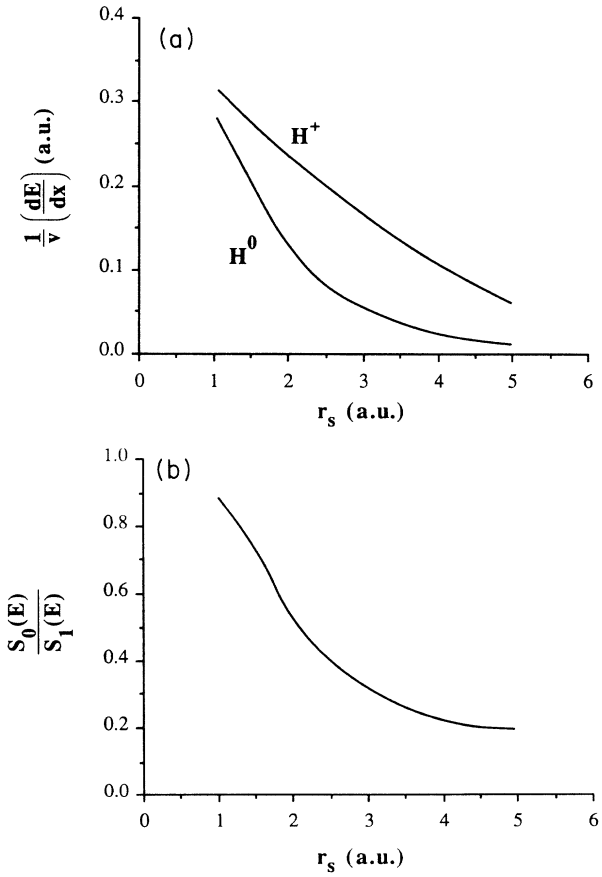

FIG. 3. (a) Ratio of stopping power and impact velocity for H^+, H^0 in solids as a function of the density parameter of the electron gas r_s. An appropriate choice for Au is $r_s\approx 1.5$. (b) Ratio of stopping power for H^0 and H^+ in solids as a function of the density parameter of the electron gas r_s.

model for the stopping power for protons with more sophisticated treatments of the scattering potential,[8] as self-consistent calculations like density functional, is acceptable (within 20%) for our present purpose of calculating these ratios.

III. EXPERIMENT

Our experimental setup for measuring electron emission statistics ("ES," i.e., the probabilities W_n for emission of $1,2,\ldots,n$ electrons caused by a single impact event) as well as total electron emission yields γ is shown schematically in Fig. 4. It is situated in an UHV chamber (base pressure below 5×10^{-10} mbar) and features a sputter-cleaned gold target ribbon mounted within a highly transparent cage. The target cleanness was checked by UPS studies in a separated surface-analyzing station, applying the same target cleaning procedures as during the actual investigations. For measuring ES the emitted electrons are extracted from the cage through an aperture and accelerated toward a solid state detector biased at +30 kV with respect to the target setup. All electrons emitted due to impact of a particular projectile arrive at the detector within its resolution time of 10^{-9} s. Consequently, they produce detector pulse heights proportional to their respective numbers. These pulses are amplified, transferred to ground potential, and pulse-height analyzed by a multichannel analyzer, from which the so-called ES spectra are obtained.[7]

Whereas ionized projectiles have been directly delivered from a Duoplasmatron ion source, the corresponding fast neutrals as well as H^- ions have been produced by charge transfer from suitable gas targets into the singly charged ions within a differentially pumped prechamber (meanwhile, the pressure in the main chamber always remained below 10^{-8} mbar). Production of excited metastable projectile states has been kept negligibly small for the rare gas atom beams by applying resonant capture processes, and for H^0 beams being produced by capture from Ar into protons. Still present minute $H(2s)$ fractions in the H^0 beam are completely quenched by electric fields in front of the collision chamber. H^- beams have been produced by double capture from H_2 into protons.

Whereas total electron yields γ for bombardment by positively charged ions can be directly measured from currents in the incoming ions and emitted electrons, this is not possible for neutral projectiles. We have therefore determined electron emission yields γ from electron emission statistics,[6] for which the following relations hold.

$$\sum_{n=0}^{\infty} W_n \equiv 1, \quad \gamma = \sum_{n=1}^{\infty} nW_n \ . \tag{12}$$

Considering directly measured yields for different singly charged ions together with corresponding relative ES data we found an empirical relation (13), which enabled us to determine γ for cases where a direct derivation of the total electron yield from current measurements is either impossible, (i.e., for neutral projectiles) or impracti-

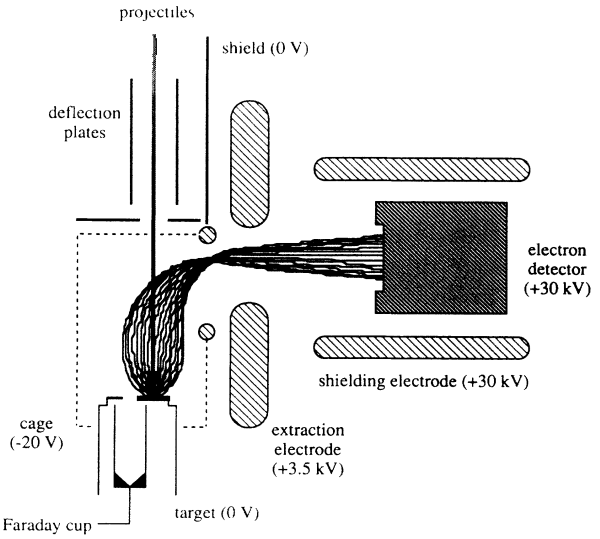

FIG. 4. Experimental setup for measuring total electron yields and electron emission statistics. Typical calculated trajectories of ejected and subsequently extracted electrons have been added.

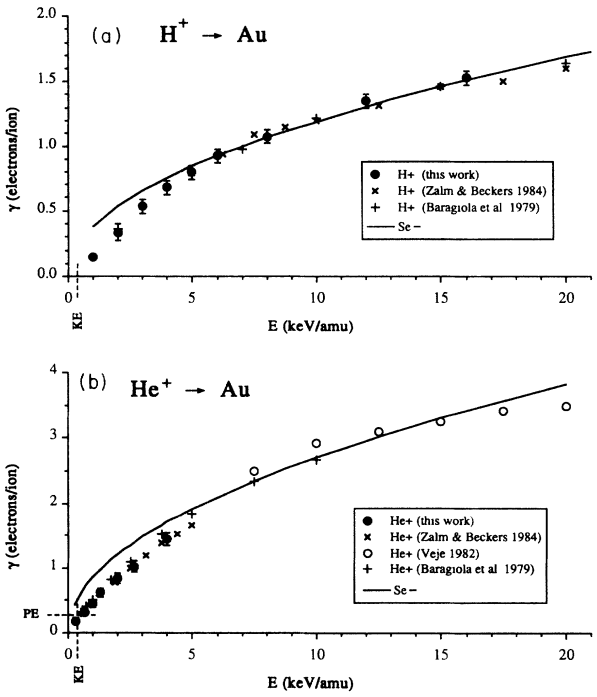

FIG. 5. (a) Electron emission yields γ for impact of H^+ (●) on clean polycrystalline gold vs E (impact energy per atomic mass unit). For comparison, data from Baragiola *et al.* (Ref. 5) (+) and Zalm and Beckers (Ref. 15) (×) for H^+ bombardment are included. The solid line shows the electronic stopping power S_e proportional to v. The vertical dashed line indicates the theoretical threshold velocity for KE. (b) Same as (a) for impact of He^+. For comparison, also data from Veje (Ref. 17) (○) for He^+ bombardment are included. In addition, the calculated PE yield according to Eq. (1) is indicated as horizontal dashed line.

TABLE I. Total electron emission yields γ for bombardment of clean polycrystalline gold with H^+, H^0, and H^-.

E (keV/amu)	γ (H^+)	γ (H^0)	γ (H^-)
1	0.15±0.02	—	—
2	0.33±0.06	0.30±0.02	—
3	0.53±0.06	0.41±0.02	0.35±0.02
4	0.68±0.05	0.53±0.03	0.52±0.03
5	0.80±0.05	0.65±0.03	0.61±0.03
6	0.93±0.05	0.74±0.04	0.70±0.04
8	1.08±0.05	0.90±0.05	0.92±0.05
12	1.35±0.05	1.12±0.06	1.27±0.06
16	1.53±0.05	0.39±0.07	1.62±0.08

cal because of too small primary particle fluxes (in particular for H^- ions):[7]

$$\gamma = 1.42\left[\frac{W_2}{W_1}\right]^2 + 1.66\frac{W_2}{W_1} . \quad (13)$$

Calculating the deviation of γ according to Eq. (13) from corresponding directly measured values, a mean error of less than ±3% is obtained for $\gamma > 0.5$, whereas for $\gamma < 0.5$ the error starts to increase, which can be attributed to errors in the current measurements.[7] The errors of relative $W_n (n \geq 1)$ are always less than ±3%,[7] from which we estimate errors of the total yields derived according to Eq. (13) to be always less than ±6%.

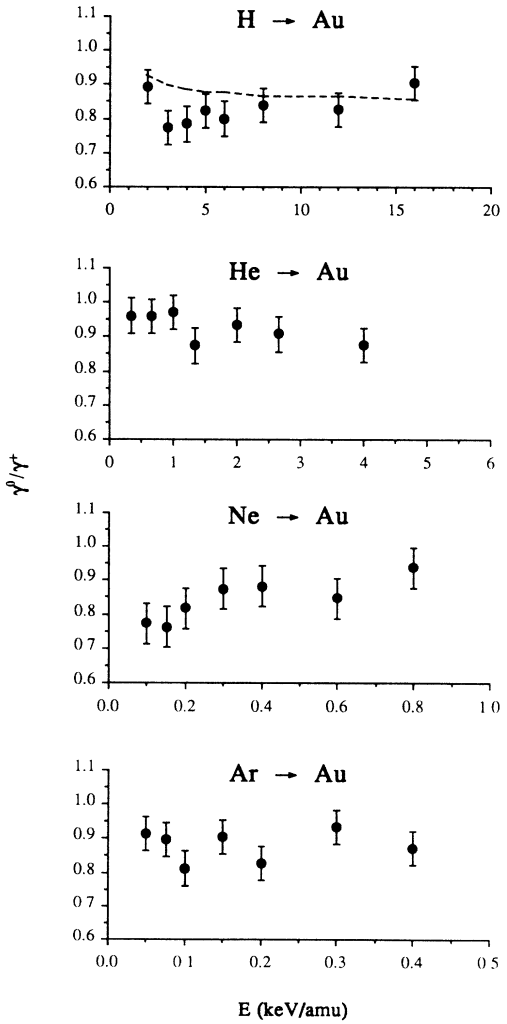

FIG. 6. Ratio of electron emission yields for impact of, respectively, neutral atoms and singly charged ions γ^0/γ^+ (●) of H, He, Ne, and Ar on clean polycrystalline gold vs E (impact energy per atomic mass unit). The dashed curve shows the theoretical prediction for $\gamma(H^0)/\gamma(H^+)$ from Eqs. (8).

IV. RESULTS

A. Comparison of measured yields with theoretical predictions

Bombardment of clean polycrystalline gold with singly charged ions at impact energies $E \geq 1$ keV causes electron emission which is clearly dominated by kinetic processes.

Figure 5(a) shows total electron yields γ for impact of H^+ on clean polycrystalline gold versus impact energy E. Corresponding data from other authors[5,15] are also shown and agree well with the present measurements within the combined experimental errors. The solid line gives an electronic stopping power $S_e \propto v$ normalized at $E = 8$ keV, showing good agreement with the measured γ values for $E \geq 6$ keV. Below $E = 6$ keV the yield becomes smaller than predicted from $S_e \propto v$. A similar deviation to smaller values than those predicted by a velocity-proportional stopping power has been found in stopping-power measurements.[16]

On the other hand, the projectile velocity corresponding to a 6-keV impact energy is about 0.5 a.u. The corresponding stopping power in Au ($r_s = 1.5$) is about 0.12 a.u. [cf. Fig. 3(a)]. This means that the proton looses about 3 eV per unit length. If this energy is lost to electronic excitations, in particular single-particle excitations

TABLE II. Total electron emission yields for bombardment of clean polycrystalline gold with He^+ and He^0.

E (keV/amu)	γ (He^+)	γ (He^0)
0.333	0.18±0.02	0.18±0.02
0.667	0.32±0.02	0.30±0.02
1.000	0.45±0.03	0.43±0.03
1.333	0.61±0.04	0.54±0.03
2.000	0.84±0.04	0.78±0.04
2.667	1.02±0.05	0.93±0.05
4.000	1.44±0.07	1.26±0.06

TABLE III. Total electron emission yields for bombardment of clean polycrystalline gold with Ne^+ and Ne^0.

E (keV/amu)	γ (Ne^+)	γ (Ne^0)
0.05	0.15±0.02	—
0.10	0.14±0.02	0.11±0.01
0.15	0.26±0.02	0.20±0.02
0.20	0.40±0.03	0.33±0.02
0.30	0.59±0.03	0.52±0.03
0.40	0.91±0.05	0.81±0.04
0.60	1.29±0.06	1.09±0.05
0.80	1.57±0.08	1.47±0.08

(electron-hole-pairs) because of no plasmon excitation, the average primary electron energy of 3 eV is certainly not very efficient to overcome the surface work function of $\Phi = 5$ eV for Au.

A similar behavior is found for bombardment of gold with He^+ [cf. Fig. 5(b)]. Although in contrast to H^+ the PE yield for He^+ is not negligible, it is still small if compared with the KE yield. The PE yield calculated from Eq. (1) is indicated in Fig. 5(b) by a horizontal line, and the vertical dashed line at $E = 0.3$ keV marks the threshold impact velocity for KE. Because of the quite considerable projectile velocity, the PE yield at this energy (see Sec. II A) is already smaller than predicted from Eq. (1). Figure 5(b) shows excellent agreement of the obtained γ data with results from other authors.[5,15] Data of Veje[17] have been included as well, because they cover the same projectile velocity range as in Fig. 5(a). Similarly as for H^+ one finds for He^+ bombardment that $\gamma \propto S_e$ for $E \geq 6$ keV/amu, as visualized by the solid line in Fig. 5(b).

B. Discussion of electronic effects

The principal purpose of this paper is to explain observed differences in KE yields for bombardment by singly charged ions and corresponding neutral atoms with equal impact velocities ("electronic effects").

One can assume that the projectile charge state changes during penetration of the target as discussed in Secs. II C and III D. Different projectile charge states cause different electronic stopping because of screening due to accompanying electrons (cf. Sec. II F). Assuming a constant screening factor k for neutral hydrogen atoms as compared to protons and a dominant equilibrium charge state of almost zero, we obtain a weakly energy-dependent ratio of the yields for these projectile species.

TABLE IV. Total electron emission yields for bombardment of clean polycrystalline gold with Ar^+ and Ar^0.

E (keV/amu)	γ (Ar^+)	γ (Ar^0)
0.025	0.07±0.01	—
0.050	0.07±0.01	0.06±0.01
0.075	0.09±0.01	0.08±0.01
0.10	0.11±0.02	0.10±0.01
0.15	0.17±0.01	0.15±0.01
0.20	0.28±0.02	0.23±0.02
0.30	0.42±0.03	0.45±0.03
0.40	0.65±0.04	0.56±0.03

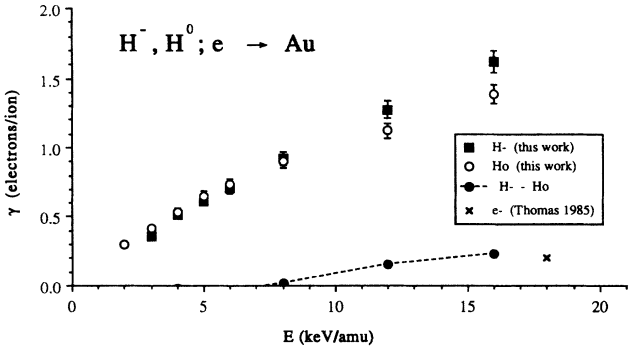

FIG. 7. Electron emission yields γ for impact of H^- (■), H^0 (○), and electrons (×) on clean polycrystalline gold vs E (impact energy per atomic mass unit). The obtained difference between yields for, respectively, H^- and H^0 bombardment is indicated by a dashed line.

Table I presents the yields for H^+ and H^0 versus impact energy. The ratio of these yields supports our predictions. γ^0/γ^+ is about 0.83±0.02. Using the theoretically obtained cross sections σ_{01} and σ_{10} (cf. Sec. II E and Fig. 2), a typical escape length of liberated electrons $L = 2$ nm,[18] a screening factor $k \approx 0.7$, and a target density for gold of $n = 6 \times 10^{28}$ m^{-3}, one can calculate the ratio γ^0/γ^+ from Eq. (8). The result varies only slightly with impact energy E within 0.94–0.86, in reasonable agreement with our measured values (cf. Fig. 6).

For He^0/He^+ bombardment we found similar electronic effects (cf. Table II). Here the ratio γ^0/γ^+ is 0.93±0.02 and practically independent of projectile energy (cf. Fig. 6).

Whereas in the so-far described cases PE was negligibly small because of the relatively high projectile velocity, this is no more the case for Ne and Ar bombardment in the here investigated energy range. The yield for bombardment with Ne^+ and Ar^+ becomes nonzero toward low projectile energy, in good agreement with the PE prediction of Eq. (1), cf. Tables III and IV. However, the ratio γ^0/γ^+ remains practically constant for Ne for $E \geq 4$ keV, and for Ar in the whole energy range.

Similar investigations have been carried out by Medved *et al.*[19] for bombardment of a clean Mo surface by Ar^0 and Ar^+, and by Mahadevan *et al.*[20] for bombardment of Mo by H^- and H^+, respectively. The latter authors assumed that the H^- ion acts like a H^0 atom. Both groups claimed lower electron emission yields for neutral atoms than for the corresponding positive ions and assigned their findings to the influence of PE. However, they also obtained a larger slope for γ^+ versus E than for γ^0, which cannot be explained from the influence of PE, since the latter decreases toward higher E.

On the other hand, it has quite often been observed that bombardment of gas-covered surfaces with neutral atoms causes higher electron yields than for the corresponding singly charged ions.[21] KE yields for gas-covered metal surfaces are in most cases considerably higher than for the corresponding clean surface. This be-

havior is generally not well understood and can probably be clarified by further measurements involving the here applied techniques.

C. Results for H^- bombardment

The second electron on the H^- ion is bound very weakly ($E_b = 0.75$ eV) in comparison to the first one. Therefore we expect that this electron is detached as soon as the ion hits the surface.[20] Figure 7 and Table I show that corresponding yields up to a projectile energy of $E = 8$ keV agree very well with those for H^0 bombardment. However, above this impact energy an extra contribution becomes apparent, which increases above the H^0 yield up to a mean value of 0.2 electrons/projectile at $E = 16$ keV. This result is in agreement with observed secondary electron emission yields $\gamma = 0.2$[22] for bombardment of Au with 10-eV electrons, with the latter involving the same impact velocity as 18-keV H^- ions. For bombardment of Mo, which features a fairly similar work function as Au, an electron threshold energy of 3.4 eV for secondary electron emission was obtained,[22] corresponding to an impact velocity of 6.5 keV for H^- ions, in satisfactory agreement with the behavior shown in Fig. 7.

On the other hand, it is well known that slow electrons impinging on metal surfaces are reflected quite efficiently.[22] Obviously this effect is of no importance in the case of H^- bombardment, because otherwise the yield difference as compared to H^0 bombardment should be much larger. Therefore we conclude that the second electron of the H^- ion is bound to the H^0 core until the first close collision with a target atom takes place, after which the electron reflection is no more as likely as in front of the surface. Nevertheless, the now "free" electrons start their own emission processes independent of the emission due to the H^0 projectiles.

V. CONCLUSIONS

In this paper we have presented a detailed study on electron emission from a clean gold surface induced by neutral atoms in comparison with singly charged ions of equal impact velocities. The measurement of electron emission statistics permitted a very sensitive and precise determination of total electron emission yields for both neutral and ionized projectile particles.

In comparison to impact of singly charged ions, the electron yields measured for neutral atom impact remain smaller over the entire range of projectile velocity by a practically constant factor. This behavior could be explained with a semiempirical model for heavy particle-induced electron emission, assuming screening of the projectile nuclei by their accompanying electron(s) during liberation of electrons inside the solid.

In particular, for bombardment with hydrogen projectiles the experimental results could be successfully explained by calculation of the charge-dependent projectile stopping power and the electron capture and loss cross sections for protons in gold. In the light of the predictions from the theoretical model it is of interest to measure yield ratios for bombardment with neutral hydrogen atoms and protons, repectively, in other target materials with lower electron density (higher r_s parameter). For such materials the stopping power ratios should be considerably smaller than for a gold target and the yield ratios should thus behave accordingly.

ACKNOWLEDGMENTS

This work has been supported by Fonds zur Förderung der wissenschaftlichen Forschung (Projekt Nr. 6381) and Kommission zur Koordination der Kernfusionsforschung at the Austrian Academy of Sciences. One of us (A.A.) gratefully acknowledges partial financial support by Eusko Jaurlaritza, Gipuzkoako Foru Aldundia, and the Spanish Comisión Asesora de Investigacion Cientifica y Technica (CAICYT). The authors are indebted to Dr. F. Aumayr for important contributions in the early stage of these measurements, to H. Kurz and M. Heim for assistance during measurements, and to M. Penalba for help in the numerical calculations.

*Also at the Departamento de Física de Materiales, Universidad del País Vasco, Apartado 1072, San Sebastián 20080, Spain.

[1]M. P. Villard, J. Physique **8**, 1 (1889).
[2]H. D. Hagstrum, Phys. Rev. **96**, 325 (1954); **96**, 336 (1954).
[3]L. M. Kishinevskii, Rad. Eff. **19**, 23 (1973).
[4]J. Schou, Phys. Rev. B **22**, 214 (1980); P. Sigmund and S. Tougaard, in *Inelastic Particle Surface Collisions*, Vol. 17 of *Springer Series in Chemical Physics*, edited by E. Taglauer and W. Heiland (Springer-Verlag, Berlin, 1981), pp. 2ff; J. Schou, Scan, Micro. **2**, 607 (1988).
[5]R. A. Baragiola, E. V. Alonso, and A. Oliva-Florio, Phys. Rev. B **19**, 121 (1979).
[6]K. H. Krebs, Ann. Phys. (Leipzig), **10**, 213 (1962).
[7]G. Lakits, F. Aumayr, and H. Winter, Rev. Sci. Instr. **60**, 3151 (1989); Phys. Lett. A **8**, 395 (1989).
[8]P. M. Echenique, I. Nagy, and A. Arnau, Int. J. Quantum Chemistry, to be published.
[9]V. Heine, in *Solid State Physics*, Vol. 24, edited by H. Ehrenreich, F. Seitz, and D. Turnbull (Academic, New York, 1970), p. 186.
[10]P. M. Echenique and F. Flores, Phys. Rev. B **35**, 8249 (1987).
[11]F. Guinea, F. Flores, and P. M. Echenique, Phys. Rev. Lett. **47**, 604 (1981).
[12]E. D. Palik, *Handbook of Optical Constants of Solids* (Academic, Orlando, Florida, 1985).
[13]F. Guinea, F. Flores, and P. M. Echenique, Phys. Rev. B **25**, 6109 (1982).
[14]P. M. Echenique, R. M. Nieminen, and R. H. Ritchie, Solid State Commun. **37**, 779 (1981).
[15]P. C. Zalm and L. J. Beckers, Philips J. Res. **39**, 61 (1984); Surf. Sci. **152/153**, 135 (1985).
[16]R. Blume, W. Eckstein, H. Verbeek, and K. Reichelt, Nucl. Instrum. Methods **194**, 67 (1982).
[17]E. Veje, Nucl. Instrum. Methods Phys. Res. B **28**, 3244 (1982).
[18]H. Kanter, Phys. Rev. B **1**, 522 (1970).

[19]Medved, P. Mahadevan, and J. K. Layton, Phys. Rev. **129**, 2086 (1963).
[20]P. Mahadevan, G. D. Magnusson, J. K. Layton, and C. E. Carlston, Phys. Rev. A **140**, 1407 (1965).
[21]C. F. Barnett and J. A. Ray, Rev. Sci. Instr. **43**, 218 (1972); P. Schackert, Z. Phys. **197**, 32 (1966).
[22]Oak Ridge National Laboratory Report No. ORNL-6088/V3, 1985 (unpublished), Vol. 3.